Brain Concentrations of Methylone and Its Metabolites after Systemic Methylone Administration: Relationship to Pharmacodynamic Effects[S]

Nicole Centazzo, Michael R. Chojnacki, Joshua S. Elmore, Raider Rodriguez, Teeshavi Acosta, Masaki Suzuki, [iD]Kenner C. Rice, Michael H. Baumann, and [iD]Marta Concheiro

Department of Sciences, John Jay College of Criminal Justice, City University of New York, New York, New York (N.C., R.R., T.A., M.C.); Designer Drug Research Unit, Intramural Research Program (IRP), National Institute on Drug Abuse (NIDA), National Institutes of Health (NIH), Baltimore, Maryland (M.R.C., J.S.E., M.H.B.); and Drug Design and Synthesis Section, IRP, NIDA, NIH, Rockville, Maryland (M.S., K.C.R.)

ABSTRACT

3,4-Methylenedioxy-*N*-methylcathinone (methylone) is a new psychoactive substance with stimulant properties and potential for abuse. Despite its popularity, limited studies have examined relationships between brain concentrations of methylone, its metabolites, and pharmacodynamic effects. The goal of the present study was 2-fold: 1) to determine pharmacokinetics of methylone and its major metabolites—4-hydroxy-3-methoxy-*N*-methylcathinone (HMMC), 3,4-dihydroxy-*N*-methylcathinone (HHMC), and 3,4-methylenedioxycathinone (MDC)—in rat brain and plasma and 2) to relate brain pharmacokinetic parameters to pharmacodynamic effects including locomotor behavior and postmortem neurochemistry. Male Sprague-Dawley rats received subcutaneous methylone (6, 12, or 24 mg/kg) or saline vehicle ($n = 16$/dose), and subgroups were decapitated after 40 or 120 minutes. Plasma and prefrontal cortex were analyzed for concentrations of methylone and its metabolites by liquid chromatography-tandem mass spectrometry. Frontal cortex and dorsal striatum were analyzed for dopamine, 5-HT, and their metabolites by high-performance liquid chromatography-electrochemical detection. Brain and plasma concentrations of methylone and its metabolites rose with increasing methylone dose, but brain methylone and MDC concentrations were greater than dose-proportional. Brain-to-plasma ratios for methylone and MDC were ≥ 3 (range 3–12), whereas those for HHMC and HMMC were ≤ 0.2 (range 0.01–0.2). Locomotor activity score was positively correlated with brain methylone and MDC, whereas cortical 5-HT was negatively correlated with these analytes at 120 minutes. Our findings show that brain concentrations of methylone and MDC display nonlinear accumulation. Behavioral and neurochemical effects of systemically administered methylone are related to brain concentrations of methylone and MDC but not its hydroxylated metabolites, which do not effectively penetrate into the brain.

SIGNIFICANCE STATEMENT

Behavioral and neurochemical effects of methylone are related to brain concentrations of methylone and its metabolite MDC but not its hydroxylated metabolites, 4-hydroxy-3-methoxy-*N*-methylcathinone and 3,4-dihydroxy-*N*-methylcathinone, which do not effectively penetrate into the brain. Methylone and MDC display nonlinear accumulation in the brain, which could cause untoward effects on serotonin neurons in vulnerable brain regions, including the frontal cortex.
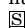
Introduction

In the past decade, nonmedical (i.e., recreational) drug markets worldwide have seen an increase in the availability of stimulant-like new psychoactive substances, including synthetic cathinones. These substances are chemically similar to amphetamines, and they have been sold as "bath salts" or "research chemicals" to evade drug control legislation in the United States and elsewhere (Baumann et al., 2013; Madras, 2016). In 2011, the most prevalent synthetic cathinones—methylone, mephedrone, and 3,4-methylenedioxypyrovalerone—were placed into emergency schedule I control by the US Drug Enforcement Administration (DEA), and the substances were permanently scheduled in 2013 (Drug Enforcement Administration (DEA), 2013). The first forensic identifications of methylone occurred in 2009 with four case reports, but serious drug exposures increased markedly in the following years,

ABBREVIATIONS: DEA, Drug Enforcement Administration; HHMC, 3,4-dihydroxy-*N*-methylcathinone; 5-HIAA, 5-hydroxyindoleacetic acid; 5-HT, 5-hydroxytryptamine or serotonin; HMMC, 4-hydroxy-3-methoxy-*N*-methylcathinone; LC-MSMS, liquid chromatography-tandem mass spectrometry; MDC, 3,4-methylenedioxycathinone; MDMA, 3,4-methylenedioxy-*N*-methylamphetamine; methylone, 3,4-methylenedioxy-*N*-methylcathinone; NIDA, National Institute on Drug Abuse; SMBS, sodium metabisulfite.

reaching a peak of 3976 case reports in 2013 (Drug Enforcement Administration (DEA), 2019). In more recent times, methylone and its analogs (e.g., pentylone) are found as adulterants in counterfeit ecstasy pills sold as the club drug 3,4-methylenedioxy-*N*-methylamphetamine (MDMA), and therefore, many drug users consume these compounds unknowingly (Oliver et al., 2019).

Methylone is the β-keto analog of MDMA, and not surprisingly, it produces similar pharmacological effects to MDMA (De Felice et al., 2014; Baumann et al., 2018). More specifically, methylone acts as a substrate-type releasing agent at high-affinity transporters for dopamine, norepinephrine, and 5-HT in rat brain tissue and in cells transfected with human transporters (Baumann et al., 2012; Eshleman et al., 2013; Simmler et al., 2013). The monoamine-releasing effects of methylone produce elevations in extracellular dopamine and 5-HT in brain reward pathways, as measured by in vivo microdialysis (Schindler et al., 2016; Elmore et al., 2017). Drug self-administration studies in rats demonstrate that methylone exhibits reinforcing properties, which suggests the drug has abuse potential (Watterson et al., 2012; Vandewater et al., 2015).

In humans, methylone is metabolized by CYP2D6, with minor contributions from CYP1A2, CYP2B6, and CYP2C19 (Pedersen et al., 2013), whereas in rats, the precise cytochrome(s) responsible are not well established but might involve CYP2D1, the rat isoform of CYP2D6 (Malpass et al., 1999). Similar to MDMA, methylone is metabolized via two distinct pathways in the liver (see Fig. 1): 1) *O*-demethylenation to form 3,4-dihydroxy-*N*-methylcathinone (HHMC), which is rapidly converted to 4-hydroxy-3-methoxy-*N*-methylcathinone (HMMC), and 2) *N*-demethylation to form 3,4-methylenedioxy-cathinone (MDC) or normethylone. It is noteworthy that HMMC is the predominant metabolite of methylone in blood and plasma from both rats and humans. Phase II metabolism includes the formation of glucuronide and sulfate conjugates of the hydroxylated metabolites HHMC and HMMC (Kamata et al., 2006; Meyer et al., 2010). Our previous studies show that certain phase I methylone metabolites are bioactive (Elmore et al., 2017; Luethi et al., 2019). MDC and HHMC are substrate-type releasers at monoamine transporters in vitro, but only MDC produces significant elevations in brain extracellular dopamine and 5-HT in vivo. The reason why HHMC lacks bioactivity in vivo is not known but could be related to poor penetration across the blood-brain barrier as a result of its rapid conjugation in the bloodstream or higher polarity when compared with methylone.

Severe clinical side effects have been reported from the misuse of methylone, such as aggressive behavior, psychosis, hyperthermia, seizures, and even death (Cawrse et al., 2012; Ellefsen et al., 2015), but limited studies have examined relationships between methylone pharmacokinetics, metabolism, and its pharmacodynamic effects. Controlled administration studies with methylone and other new psychoactive substances in humans are limited as a result of ethical constraints, so pharmacokinetic studies in animal models fill a critical void. Several research groups have investigated the pharmacokinetics and pharmacodynamics of methylone in rodent models (López-Arnau et al., 2013; Elmore et al., 2017; Grecco et al., 2017; Štefková et al., 2017). In particular, López-Arnau et al. (2013) examined pharmacokinetics of methylone in rats, and their findings suggest that metabolites may contribute to
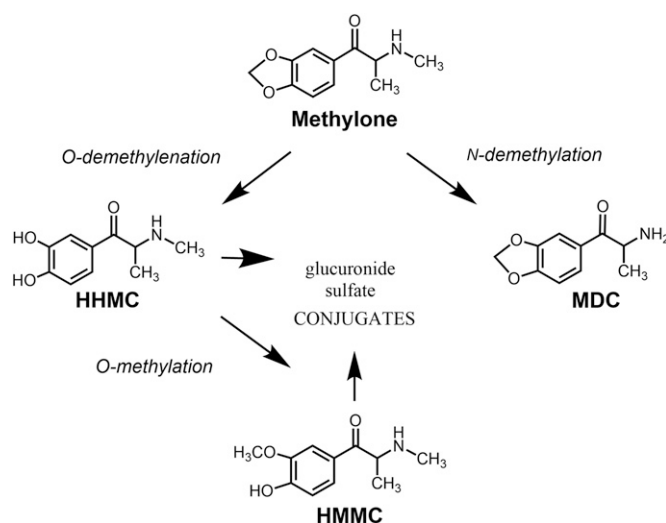

Fig. 1. Metabolism of methylone. Shown are chemical structures of methylone and its main metabolites: HHMC, HMMC, and MDC.

pharmacodynamic effects of the drug in vivo. Given the aforementioned information, the goal of the present study was 2-fold: 1) to determine the pharmacokinetics of methylone and its three major metabolites—HMMC, HHMC, and MDC—in rat brain and plasma and 2) to relate brain pharmacokinetic parameters to acute pharmacodynamic effects including locomotor behavior and postmortem neurochemistry.

Materials and Methods

Drugs, Chemicals, and Reagents. (±)-3,4-Methylenedioxy-*N*-methylcathinone (methylone) for animal studies was acquired from the National Institute on Drug Abuse (NIDA), Drug Supply Program (Rockville, MD). For analytical procedures, methylone (1 mg/ml in methanol) and its deuterated standard methylone-d_3 (100 μg/ml in methanol) were obtained from Cerilliant (Round Rock, TX). As reported by Ellefsen et al. (2015), the methylone metabolites MDC, HHMC, and HMMC were synthesized and purified by the Drug Design and Synthesis Section of the NIDA Intramural Research Program (Baltimore, MD). The monoamine standards for dopamine, 3,4-dihydroxyphenylacetic acid, homovanillic acid, 5-HT, and 5-hydroxyindole-acetic acid (5-HIAA) were obtained from Sigma-Aldrich (St. Louis, MO).

Liquid chromatography-mass spectrometry–grade acetonitrile, EDTA, formic acid, isopropanol, methanol, and sodium metabisulfite (SMBS) were obtained from Thermo Fisher Scientific (Fair Lawn, NJ). BG100 liquid β-glucuronidase from Red Abalone *Haliotis rufescens* (>100 kU/ml) was purchased from Kura Biotec (Inglewood, CA), and 4-methylcatechol was from Sigma-Aldrich (Milwaukee, WI). Hydrochloric acid (HCl) 36.5%–38% was obtained from J. T. Baker Chemical Company (Phillipsburg, NJ). Brains from drug-naïve male Sprague-Dawley rats were acquired from BioIVT (Hicksville, NY) and used for development of the method to quantify methylone in brain tissue. The 2-ml, 1.4-mm ceramic beads were obtained from Thermo Fisher Scientific, and 10-ml, 100 × 16 mm polypropylene tubes were purchased from Sarstedt Inc. (Newton, NC).

Animals, Dosing Regimen, and Tissue Collection. Male Sprague-Dawley rats (300–400 g), purchased from Envigo (Frederick, MD), were double-housed under conditions of controlled temperature (22 ± 2°C) and humidity (45% ± 5%) with ad libitum access to food and water. Lights were on between 7:00 AM and 7:00 PM. The Institutional Animal Care and Use Committee of the NIDA Intramural Research Program approved the animal experiments, and all procedures

were carried out in accordance with the National Institutes of Health Guide for the Care and Use of Laboratory Animals. Vivarium facilities were fully accredited by the Association for Assessment and Accreditation of Laboratory Animal Care. Experiments were designed to minimize the number of animals included in the study.

At 1 week prior to drug treatments, rats were single-housed. On the day of the experiment, groups of rats received subcutaneous methylone (6, 12, or 24 mg/kg) or its saline vehicle ($n = 16$/dose) and were returned to their home cages; subgroups were subsequently killed by decapitation at 40 or 120 minutes postinjection. These particular time points were chosen for tissue collection based on our previous study, which showed plasma MDC concentrations peak at 30–40 minutes postinjection, whereas plasma HMMC concentrations peak much later, at 90–120 minutes (Elmore et al., 2017). Injections were carried out in the vivarium, whereas decapitation was carried out in a separate necropsy room. Trunk blood was collected; brains were rapidly removed from the skull; and tissue from prefrontal cortex, frontal cortex, and dorsal striatum was dissected on ice. Plasma and brain tissue were stored frozen at $-80°C$ until the time of analysis.

Assessment of Locomotor Behavior and Body Temperature. Just prior to decapitation, each rat was observed for 1 minute in its home cage to discern locomotor behavior, and core body temperature was measured. Behavior was scored using a numerical scale: 1 = asleep or still; 2 = in-place activities; 3 = locomotion, rearing, or sniffing; 4 = any two (locomotion, rearing, or sniffing); 5 = 10 seconds of continuous sniffing without locomotion or rearing; 6 = 10 seconds of continuous sniffing with locomotion or rearing; 7 = 5 seconds of patterned sniffing; 8 = 10 seconds of patterned sniffing. Patterned sniffing was defined as any repeated head motion (e.g., up and down "head bobbing") that occurred simultaneously with sniffing behavior. This behavioral scale is sensitive to dose-related changes in motor activation caused by psychomotor stimulants (Baumann et al., 1993; Elmore et al., 2017). The behavioral observer was blinded to the experimental condition. After the observation period, rats were removed from their cages, and core body temperature was measured via insertion of a RET-2 probe (Physitemp Instruments, Clifton, NJ) into the colon. Rats were then transported in their home cages to the necropsy room, where they were decapitated.

Monoamine and Metabolite Analysis in Rat Brain. Brain tissue from the frontal cortex and dorsal striatum was analyzed for dopamine, 3,4-dihydroxyphenylacetic acid, homovanillic acid, 5-HT, and 5-HIAA via high-performance liquid chromatography with electrochemical detection. Tissue samples were weighed, homogenized by ultrasonication in 0.1 N perchloric acid, and centrifuged at $16,600g$ for 18 minutes at 4°C in an Eppendorf 5415R refrigerated centrifuge by Marshall Scientific (Hampton, NH). Aliquots of the supernatant were injected onto a Sunfire C18 high-performance liquid chromatography column (150 × 4.6 mm, 3.5-μm particles, 100-Å pore size) (Waters Millipore, Milford, MA) linked to a coulometric detector (ESA Model Coulochem III; Dionex, Chelmsford, MA). Mobile phase consisting of 50 mM sodium phosphate monobasic, 250 μM Na$_2$EDTA, 0.03% sodium octane sulfonic acid, and 25% methanol (pH = 2.75) was recirculated at 0.9 ml/min. Known monoamine standards, ranging in concentration from 10 to 1000 pg/μl, were assayed along with each set of samples. Data were acquired by a Waters Empower software system (Waters Millipore), and peak heights of unknowns were compared with those of standards. The lower limit of assay sensitivity (3 times baseline noise) was 30 pg/20 μl sample.

Methylone and Metabolites Analysis in Rat Plasma. Plasma samples were analyzed by liquid chromatography-tandem mass spectrometry (LC-MSMS) as previously described by Ellefsen et al. (2015). Specifically, 20 μl of 250 mM SMBS, 10 μl of 250 mM EDTA, 50 μl of internal standard (methylone-d$_3$) at 100 ng/ml, and 100 μl rat plasma were mixed in 1.5-ml microcentrifuge tubes and gently vortexed. After enzymatic hydrolysis (10 μl of β-glucuronidase, incubation at 50°C, 1 hour), 20 μl of 4-methylcathechol and 10 μl of perchloric acid were mixed with each sample. The samples were extracted using mixed-mode cation exchange solid-phase extraction. The eluent was acidified

with 100 μl of 1% HCl in methanol and evaporated to dryness in a Turbovap (Biotage, Charlotte, NC). In total, 200 μls of 0.1% formic acid in water was used for reconstitution, and the solution was transferred to injection vials. An LC-MSMS system with a Nexera ultra high performance chromatographic system coupled to a triple quadrupole LCMS-8050 from Shimadzu (Columbia, MD) was employed for the instrumental analysis. The chromatographic separation was performed using a Synergi Polar-RP liquid chromatography column (100 × 2 mm, 2.5-μm particles, 100-Å pore size) (Phenomenex, Torrance, CA), and the mobile phase in gradient mode was a combination of 0.1% formic acid in water (mobile phase A) and 0.1% formic acid in acetonitrile (mobile phase B). Mass spectrometer data were collected in positive electrospray ionization mode with two multiple reaction monitoring transitions per analyte (Supplemental Table 1). The method was linear from 0.5 (methylone, HMMC, and MDC) or 10 (HHMC) to 1000 ng/ml. Validation details are described in Ellefsen et al. (2015). If a plasma sample was quantified above the upper limit of quantification (1000 ng/ml), the sample was diluted 1:10 with blank rat plasma and reanalyzed. Once the diluted sample was quantified within the calibration range, the final concentration was obtained by multiplying the measured concentration of the diluted sample by the dilution factor.

Methylone and Metabolite Analysis in Rat Brain. Prefrontal cortical tissue from each rat was weighed and transferred into a bead mill tube containing ceramic beads and 500 μl of 7.5 mM SMBS, 7.5 mM EDTA, in 10 mM formic acid (SMBS-EDTA-Formic acid mixture). The samples were homogenized on a Bead Ruptor Elite bead mill homogenizer by OMNI International (Kennesaw, GA). The homogenization program consisted of one cycle lasting 20 seconds at a speed of 4.85 m/s. After centrifugation ($6200g$, 5 minutes), 25 μl internal standard (methylone-d$_3$) at 100 ng/ml was added, and the enzymatic hydrolysis was performed (10 μl of β-glucuronidase, incubation at 50°C, 1 hour). After adding 20 μl of 4-methylcatechol to each sample, 800 μl of cold acetonitrile was used for protein precipitation. In total, 100 μl of 1% HCl in methanol was added to the supernatant, and samples were evaporated to dryness. Reconstitution was performed by adding 200 μl of mobile phase A, and the sample was transferred into a nanoFilter Vial 0.2-μm polyvinylidene difluoride with red screw cap (Thomson Instrument Company, Oceanside, CA) before being analyzed by LC-MSMS as described for the plasma samples (injection volume 20 μl). The method was linear, from 5 to 1000 ng/g for all compounds. Validation parameters are summarized in Supplemental Tables 2–4. If a brain sample quantified above the upper limit of quantification (1000 ng/g), the brain homogenate was diluted at 1:10 or 1:100 with the SMBS-EDTA-Formic acid mixture and reanalyzed. Once the diluted sample quantified within the calibration range, the final concentration was obtained by multiplying the measured concentration of the diluted sample by the dilution factor.

Data Analysis and Statistics. Data collected from the analysis of drug and metabolite concentrations, locomotor activity scores, body temperature, and neurotransmitter levels were tabulated, analyzed, and graphed with GraphPad Prism (version 7; GraphPad Software, La Jolla, CA). For the pharmacokinetic findings, two-way ANOVA (dose × matrix) followed by Sidak's multiple comparison test was performed to compare plasma versus brain concentrations of analytes. As a means to assess the potential for nonlinear accumulation of analytes, two-way ANOVA (dose × condition) followed by Sidak's test was used to compare predicted versus observed brain concentrations of methylone and MDC at each time point. Predicted brain concentrations at the doses of 12 and 24 mg/kg were calculated by multiplying measured analyte concentrations after 6 mg/kg methylone by a factor of 2 and 4, respectively. Pharmacodynamic findings were examined by one-way ANOVA (dose), followed by Bonferroni's post hoc test. A correlation matrix that included brain concentrations of methylone and MDC, neurotransmitter levels from the frontal cortex and dorsal striatum, locomotor activity scores, and core temperature was created and

TABLE 1

Plasma concentrations (ng/ml) of methylone, MDC, HHMC, and HMMC from rats receiving subcutaneous methylone at 6, 12, and 24 mg/kg.
Samples were collected at 40 or 120 min postinjection. Data are means ± S.E.M. for $N = 8$ rats per group.

Dose (mg/kg)	Collection Time	Methylone	MDC	HHMC	HMMC
	min		*ng/ml*		
6	40	687.4 ± 37	234.6 ± 10.8	290 ± 22.6	201.6 ± 12.5
	120	133.4 ± 9.4	164 ± 10.7	157.9 ± 12.8	248.5 ± 41.8
12	40	1037.3 ± 27.6	491.7 ± 17.5	432.8 ± 55	244.5 ± 17
	120	506.5 ± 40.2	384.5 ± 12.6	260 ± 36.7	334.8 ± 30.4
24	40	3749.9 ± 132.2	1007.6 ± 34.5	809.8 ± 71.2	402.9 ± 16.8
	120	1230.8 ± 196.5	875.3 ± 31.1	686.7 ± 45.6	537.8 ± 38.8

subsequently analyzed by Pearson's tests and linear regression analyses. In all the statistical analyses, $P < 0.05$ was considered significant.

Results

Pharmacokinetics of Methylone and Its Metabolites. A total of 48 brain and plasma samples from rats receiving subcutaneous methylone (three doses), collected at 40 or 120 minutes postinjection (two time points), were analyzed with the described LC-MSMS procedure ($n = 8$ rats/dose at each time point). The limits of quantification in brain and plasma were 5 ng/g and 0.5 ng/ml, with the exception of HHMC in plasma, which displayed a limit of quantification of 10 ng/ml. The plasma concentrations of analytes are summarized in Table 1, whereas brain concentrations are summarized in Table 2. In general, concentrations of methylone and its metabolites increased in both matrices as the dose administered was increased.

Figure 2 depicts the brain and plasma concentrations of methylone and MDC at the 40- and 120-minute time points. A two-way ANOVA (dose × matrix) comparing brain and plasma concentrations of methylone at 40 minutes revealed significant main effects of dose ($F_{2,42} = 27.09$, $P < 0.0001$) and matrix ($F_{1,42} = 75.19$, $P < 0.0001$), with a significant dose × matrix interaction ($F_{2,42} = 17.85$, $P < 0.0001$). Similar results were found for methylone measures at 120 minutes. At all doses and time points, brain concentrations of methylone were far greater than plasma concentrations. A two-way ANOVA comparing brain and plasma concentration of MDC at 40 minutes revealed significant effects of dose ($F_{2,42} = 21.62$, $P < 0.0001$) and matrix ($F_{1,42} = 58.40$, $P < 0.001$), with a significant dose × matrix interaction ($F_{2,42} = 9.932$, $P < 0.003$). Similar results were found for MDC measures at 120 minutes. At all doses and time points, brain concentrations of MDC exceeded those measured in plasma. Figure 3 illustrates the brain and plasma concentrations of the hydroxylated metabolites HHMC and HMMC. In contrast to the findings for methylone and MDC, brain concentrations of HHMC and HMMC were extremely low in all tissue samples. A two-way ANOVA comparing the brain and plasma concentration of HHMC at 40 minutes revealed significant effects of dose ($F_{2,42} = 25.90$, $P < 0.0001$) and matrix ($F_{1,42} = 244.6$, $P < 0.0001$), with a significant dose × matrix interaction ($F_{2,42} = 21.18$, $P < 0.0001$). Similar results were found for HHMC at 120 minutes. At all doses and time points, plasma concentrations of HHMC were significantly greater than brain concentrations. A two-way ANOVA comparing brain and plasma concentration of HMMC at 40 minutes revealed significant effects of dose ($F_{2,41} = 56.73$, $P < 0.0001$) and matrix ($F_{1,41} = 694$, $P < 0.0001$), with a significant dose × matrix interaction ($F_{2,41} = 26.98$, $P < 0.0001$). Similar results were found for HMMC at 120 minutes. At all doses and time points, plasma concentrations of HMMC far exceeded those measured in brain.

The data in Table 3 summarize brain-to-plasma ratios for all analytes. Methylone and MDC displayed brain-to-plasma ratios ≥ 3 (range 3–14), whereas HHMC and HMMC had ratios ≤ 0.2 (range of 0.01–0.2). These results confirm that methylone and its *N*-demethylated metabolite MDC freely cross the blood-brain barrier to reach the brain, whereas HHMC and HMMC do not. To investigate the possible reasons underlying the lack of hydroxylated metabolites reaching the brain, we explored the presence of glucuronide or sulfate conjugates in both plasma and brain. Briefly, we compared analyte concentrations in plasma and brain samples, which were subjected to two separate analytical procedures, one that involved sample hydrolysis to cleave conjugated metabolites and another that did not. In the brain, no phase II metabolites were detected for any of the metabolites. In plasma, HMMC and HHMC were mainly present as conjugates. The percentage of HMMC in conjugated form ranged from 47.6% to 95.7% (median 84.6%), and the percentage of HHMC as conjugated metabolite ranged from 49.2% to 99.8% (median 87.6%). These results show that HHMC and HMMC are predominantly

TABLE 2

Brain concentrations (ng/g) of methylone, MDC, HHMC, and HMMC from rats receiving subcutaneous methylone at 6, 12, and 24 mg/kg collected at 40 or 120 min postinjection.
Data are means ± S.E.M. for $N = 8$ rats per group.

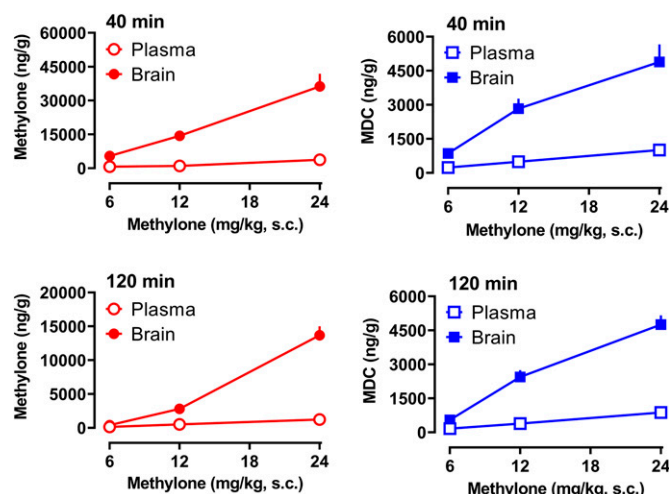| Dose (mg/kg)	Collection Time	Methylone	MDC	HHMC	HMMC
	min		*ng/g*		
6	40	5404.6 ± 779	857 ± 122.7	3.9 ± 1	16.8 ± 1.7
	120	403.7 ± 62.3	545.4 ± 80.9	1.1 ± 0.8	13.9 ± 1.8
12	40	14,357.3 ± 1324.4	2832.5 ± 437.7	12 ± 1.9	25.7 ± 4
	120	2796.8 ± 704.5	2441 ± 303.4	9.4 ± 1.8	34.5 ± 4.1
24	40	36,222.9 ± 5617.2	4886.5 ± 770.3	30.3 ± 3.5	54.1 ± 6.6
	120	13,671.8 ± 1339.3	4750.2 ± 406.3	23.8 ± 3.5	59.7 ± 7.6

Fig. 2. Plasma and brain concentrations of methylone and MDC at early and late time points (40 and 120 minutes) after subcutaneous methylone injections (6, 12, and 24 mg/kg). Data are means ± S.E.M. for n = 8 rats per group.

present as conjugates in plasma, and these conjugates do not cross the blood-brain barrier.

Data from our previous study suggested that methylone concentrations in plasma may exhibit nonlinear accumulation, in which circulating drug concentrations are greater than dose-proportional (Elmore et al., 2017). Therefore, we compared the predicted concentrations of methylone and MDC in brain tissue to their actual observed concentrations. Data in Fig. 4 show the predicted versus observed concentrations for methylone and MDC in brain. A two-way ANOVA (dose × condition) comparing predicted versus observed brain concentrations of methylone at the 40-minute time point revealed significant main effects of dose ($F_{2,42} = 32.49$, $P < 0.0001$) and condition ($F_{1,42} = 6.05$, $P < 0.01$), in which observed methylone concentrations were significantly greater than predicted at the dose of 24 mg/kg methylone ($P < 0.05$ Sidak's test). Similar results were found for the 120-minute time point, at which the
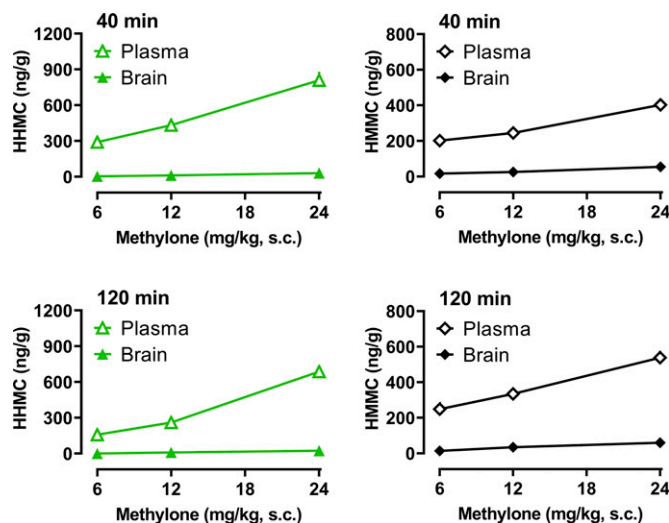

Fig. 3. Plasma and brain concentrations of HHMC and HMMC at early and late time points (40 and 120 minutes) after subcutaneous methylone injections (6, 12, and 24 mg/kg). Data are means ± S.E.M. for n = 8 rats per group.

observed concentration of methylone was significantly greater than the predicted concentration at a dose of 24 mg/kg. A two-way ANOVA comparing the predicted versus observed brain concentrations of MDC at the 40-minute time point revealed significant main effects of dose ($F_{2,42} = 29.45$, $P < 0.001$) and condition ($F_{1,42} = 5.93$, $P < 0.01$), but the predicted and observed concentrations did not differ significantly at any dose. A similar analysis of MDC concentrations at 120 minutes found significant main effects of dose ($F_{2,42} = 64.36$, $P < 0.0001$) and condition ($F_{1,42} = 38.34$, $P < 0.0001$), in which the observed concentrations were significantly greater than predicted at doses of 12 and 24 mg/kg . The findings with MDC suggest that there is a delayed accumulation of this analyte in the brain.

Pharmacodynamic Effects of Methylone. The effects of methylone on core body temperature and locomotor behavioral score are shown in Fig. 5. Methylone administration affected temperature in a dose- and time-dependent manner, with initial hypothermia followed by delayed hyperthermia. A one-way ANOVA (dose) for temperature data demonstrated that methylone significantly affected body temperature at the 40-minute time point ($F_{3,28} = 11.90$, $P < 0.0001$), with modest hypothermia occurring after doses of 6 and 12 mg/kg. At the 120-minute time point, methylone significantly affected temperature ($F_{3,28} = 5.734$, $P < 0.003$), with a modest but significant hyperthermia of about 0.5°C above normal observed at doses of 12 and 24 mg/kg. Methylone administration significantly altered locomotor score at both 40 minutes ($F_{3,28} = 56.36$, $P < 0.0001$) and 120 minutes ($F_{3,28} = 36.55$, $P < 0.0001$). At both time points, Bonferroni's post hoc test revealed significant increases in behavioral score after the doses of 6, 12, and 24 mg/kg when compared with saline control. Figure 6 depicts the effects of methylone on postmortem concentrations of 5-HT and dopamine in the frontal cortex. Methylone did not affect 5-HT at 40 minutes but significantly influenced 5-HT at 120 minutes ($F_{3,28} = 33.88$, $P < 0.0001$), with substantial dose-related decreases in 5-HT, which reached 60% reduction at the dose of 24 mg/kg. Methylone failed to alter dopamine concentrations in the frontal cortex. Figure 7 shows the effects of methylone on postmortem tissue 5-HT and dopamine in the dorsal striatum. Methylone had no effect on striatal 5-HT at either time point. By contrast, methylone slightly, albeit significantly, elevated striatal dopamine at both the 40-minute ($F_{3,28} = 3.73$, $P < 0.02$) and 120-minute ($F_{3,28} = 7,29$, $P < 0.001$) time points.

Correlative Relationships. We obtained pharmacokinetic and pharmacodynamic data from the same experimental subjects, which allowed us to examine potential correlative relationships among various endpoints. We were particularly interested in the relationship between brain analyte concentrations and pharmacodynamic effects. The present pharmacokinetic findings revealed the absence of hydroxylated metabolites in the brain, so all correlation analyses were confined to brain concentrations of methylone and MDC. Figure 8 depicts the correlations between brain concentrations of methylone and body temperature or behavioral score. At the 40-minute time point, brain methylone was positively correlated with both temperature (Pearson's r = 0.6751, $P < 0.0005$) and behavioral score (r = 0.6985, $P < 0.0001$). At 120 minutes, methylone was not correlated with temperature (r = 0.3567, N.S.) but did correlate with behavioral score (r = 0.7841, $P < 0.0001$). Figure 9 shows that brain MDC concentrations were

TABLE 3
Brain-to-plasma concentration ratios for methylone, MDC, HHMC, and HMMC from rats receiving subcutaneous methylone at 6, 12, and 24 mg/kg.
Data are means ± S.E.M. for N = 8 rats per group.

Dose (mg/kg)	Collection Time	Methylone	MDC	HHMC	HMMC
	min				
6	40	7.66 ± 0.76	3.76 ± 0.64	0.01 ± 0	0.08 ± 0.01
	120	3 ± 0.4	3.34 ± 0.46	0.01 ± 0	0.06 ± 0.01
12	40	14 ± 1.44	5.77 ± 0.86	0.03 ± 0.01	0.11 ± 0.02
	120	5.4 ± 1.08	6.35 ± 0.76	0.04 ± 0.01	0.1 ± 0.01
24	40	9.64 ± 1.37	4.88 ± 0.80	0.07 ± 0.03	0.20 ± 0.09
	120	12.39 ± 1.72	5.48 ± 0.52	0.04 ± 0.01	0.12 ± 0.02

positively correlated with body temperature (r = 0.6118, P < 0.0015) and behavioral score (r = 0.6688, P < 0.0004) at 40 minutes postinjection, and similar positive correlations were observed at the 120-minute time point.

Figure 10 illustrates the correlations between brain methylone concentration and cortical 5-HT or dopamine. Brain concentrations of methylone did not correlate with either cortical neurotransmitter at 40 minutes. However, at the 120-minute time point, methylone was negatively correlated with cortical 5-HT (r = −0.6701, P < 0.0003). Figure 11 shows the correlations between MDC concentrations and cortical 5-HT or dopamine. Brain concentrations of MDC did not correlate with either neurotransmitter at the 40-minute time point, but at 120 minutes, there was a significant negative correlation between MDC and 5-HT (r = −0.7597, P < 0.0001). No correlations were found when examining relationships among methylone, MDC, and striatal neurotransmitters.

Discussion

A primary aim of the present study was to quantify brain and plasma concentrations of methylone and its metabolites after systemic methylone administration to male rats. In general, methylone and metabolite concentrations rose in parallel with increasing doses of methylone administered, but brain methylone and MDC concentrations were greater than dose-proportional at the highest dose administered. Methylone and MDC displayed brain-to-plasma ratios ≥ 3 (range 3–12), whereas HHMC and HMMC had brain-to-plasma ratios ≤ 0.2 (range 0.01–0.2). These findings demonstrate that methylone and MDC freely penetrate into the central nervous system but hydroxylated metabolites do not. A secondary aim of the study was to relate brain analyte concentrations with acute pharmacodynamic effects of methylone. In this regard, locomotor activity score was positively correlated with brain concentrations of methylone and MDC, whereas postmortem 5-HT levels in the cortex were negatively correlated with these same analytes. Overall, the findings show that acute pharmacodynamic effects of methylone are likely related to brain concentrations of the parent compound and its N-demethylated metabolite.

It is notable that we found evidence for nonlinear accumulation of methylone and MDC in the brain. Elmore et al. (2017) reported nonlinear kinetics for methylone in plasma, whereas López-Arnau et al. (2013) found no evidence for the phenomenon. Here, we report the first dose-effect investigation of methylone and metabolite concentrations in the brain. The doses of methylone we employed were chosen based on our previous study (Elmore et al., 2017), in which we observed higher-than-predicted concentrations of methylone in plasma after subcutaneous administration of 12 mg/kg. The current findings show that nonlinear accumulation of methylone and MDC
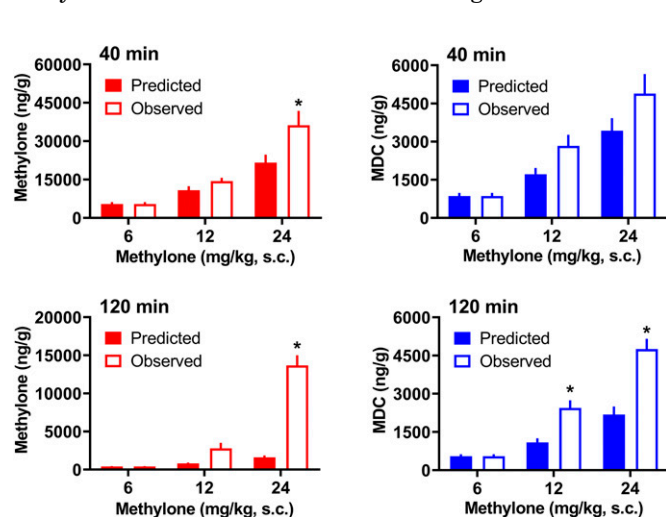

Fig. 4. Predicted vs. observed brain concentrations of methylone and MDC at early and late time points (40 and 120 minutes). Predicted concentrations at doses of 12 and 24 mg/kg were calculated by multiplying the observed values at 6 mg/kg by a factor of 2 and 4, respectively. Data are means ± S.E.M. for n = 8 rats per group. Asterisks represent significant difference compared with predicted group (P < 0.002).
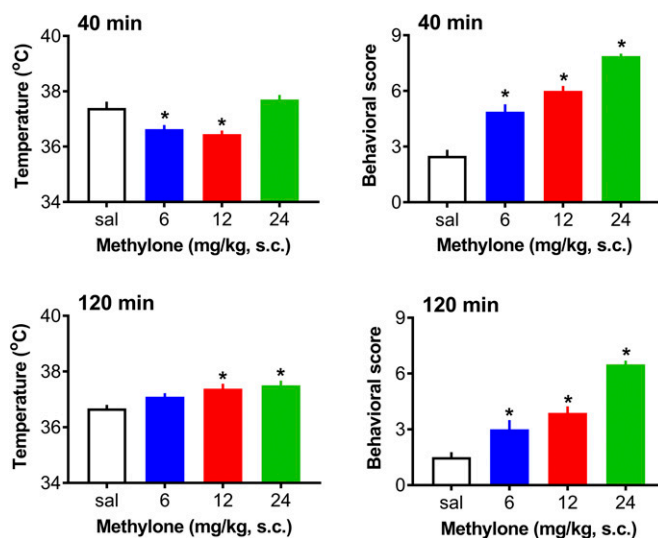

Fig. 5. Effects of subcutaneous methylone administration (dose of 6, 12, and 24 mg/kg) on body temperature and behavioral score at 40 and 120 minutes postinjection. Data are means ± S.E.M. for n = 8 rats per group. Asterisks represent significant differences compared with saline-treated control group (sal).
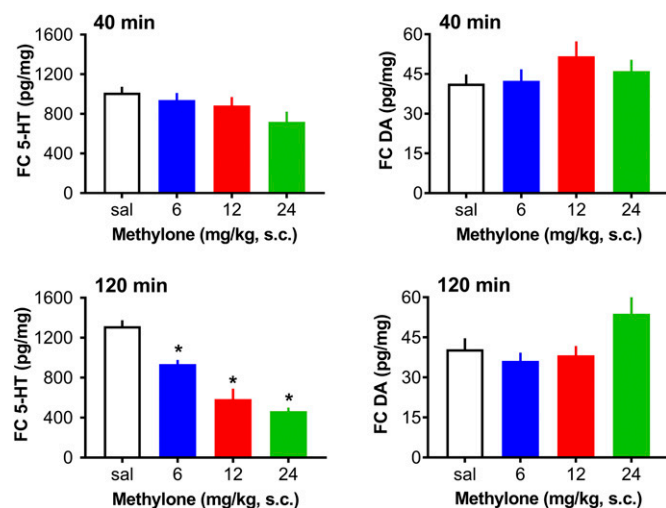
Fig. 6. Effect of subcutaneous methylone administration (6, 12, and 24 mg/kg) on postmortem levels of dopamine (DA) and serotonin (5-HT) from frontal cortex at 40 minutes and 120 minutes postinjection. Data are means ± S.E.M. for $n = 8$ rats per group. Asterisks represent significant differences compared with saline-treated control group (sal).

Fig. 8. Correlations between brain methylone concentrations and body temperature or behavioral score at 40 and 120 minutes postinjection.

occurs in the brain at higher drug doses, and this effect is more robust after 120 minutes compared with 40 minutes. Our data are consistent with the notion that methylone induces a dose- and time-dependent inhibition of CYP2D1 (the rat isoform of CYP2D6 in humans), the chief enzyme responsible for biotransformation of methylone. Indeed, Pedersen et al. (2013) found that methylone inhibits CYP2D6, with a Ki of 15 μM, which translates to ∼3000 ng/g, a concentration that is achieved in rat brain tissue after the doses of 12 and 24 mg/kg methylone (see Table 2). We hypothesize that methylone is capable of inactivating CYP2D1 in rats in a manner analogous to the effect of MDMA on CYP2D6 in humans (de la Torre et al., 2004), and subsequent studies should address this hypothesis. From a clinical perspective, the nonlinear kinetics of methylone might be a contributing factor to the adverse effects of the drug reported after high-dose exposure in humans (Cawrse et al., 2012; Ellefsen et al., 2015). Similar toxicities
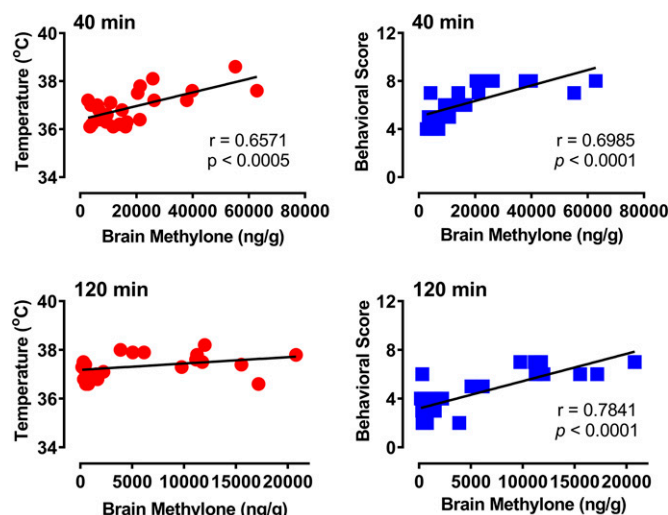
have been reported in rats self-administering large doses of methylone (Gannon et al., 2018, 2019).

The collection of brain tissue and plasma from the same rats made it possible to determine brain-to-plasma ratios for methylone and its metabolites. Our results reveal that methylone and MDC are readily able to cross the blood-brain barrier (brain-to-plasma ratios from 3 to 14), whereas HHMC and HMMC do not (brain-to-plasma ratio from 0.01 to 0.2). In fact, the small amounts of HHMC and HMMC detected in brain were likely related to analyte concentrations in residual blood found in postmortem brain tissue samples. Limited information is available about the distribution of methylone and its metabolites in the brain or other organs (Štefková et al., 2017). López-Arnau et al. (2013) reported a methylone brain-to-plasma ratio of 1.42 after an oral dose of 30 mg/kg methylone. In that study, the oral route of administration might explain lower concentrations of drug reaching the brain, secondary to extensive gut and hepatic metabolism of the parent compound. Štefková et al. (2017) reported that subcutaneous methylone administration yields a brain-to-serum ratio of
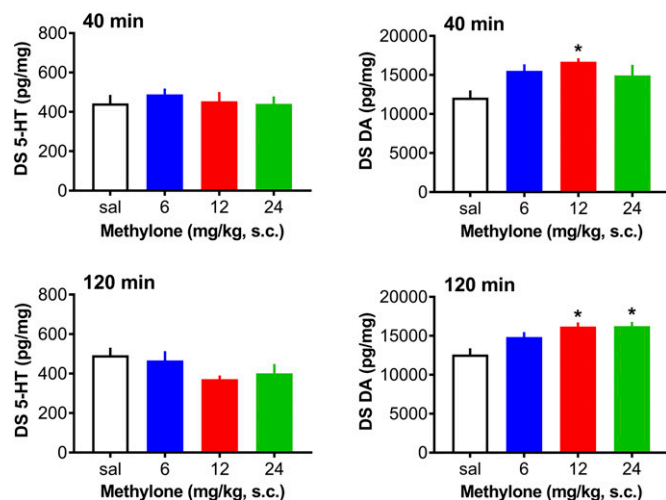

Fig. 7. Effect of subcutaneous methylone administration (6, 12, and 24 mg/kg) on postmortem levels of dopamine (DA) and serotonin (5-HT) from dorsal striatum (DS) at 40 and 120 minutes postinjection. Data are means ± S.E.M. for $n = 8$ rats per group. Asterisks represent significant differences compared with saline-treated control group (sal).
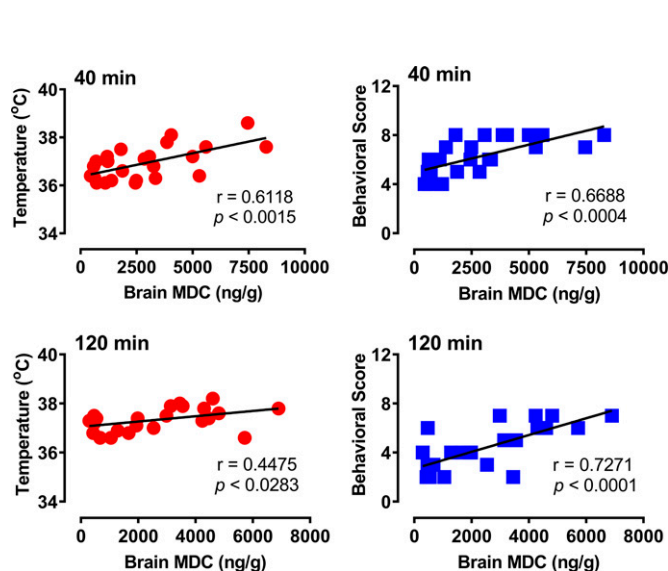

Fig. 9. Correlations between brain MDC concentrations and body temperature or behavioral score at 40 and 120 minutes postinjection.
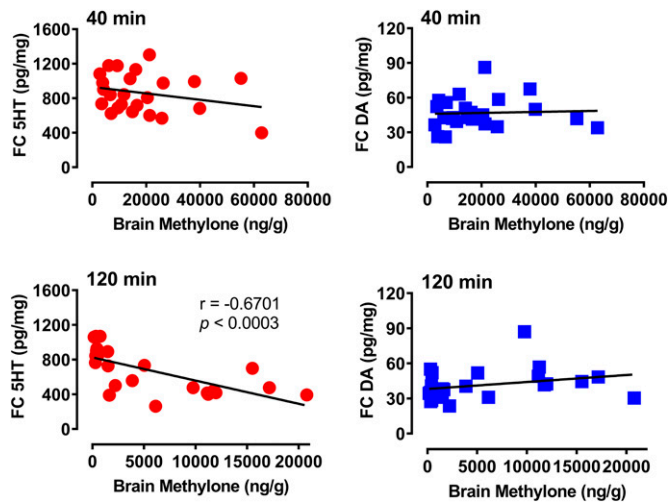
Fig. 10. Correlations between brain methylone concentrations and frontal cortical (FC) 5-HT and dopamine (DA) at 40 and 120 minutes postinjection.

7.97, whereas Grecco et al. (2017) found that subcutaneous methylone yields a brain-to-plasma ratio of 39.5. It is noteworthy that the latter finding was based on area-under-curve estimates rather than single time points. Regardless of the details, all of the available data from rats agree that methylone and MDC freely cross the blood-brain barrier. In contrast to methylone and MDC, we show that HHMC and HMMC are found at particularly low concentrations in the brain. The inability of the hydroxylated metabolites to enter the brain is most likely due to the high percentage of HHMC and HMMC conjugates in plasma, which are too polar to penetrate into the brain. Elmore et al. (2017) showed that methylone, MDC, and HHMC were substrate-type releasers at monoamine transporters in vitro, but only methylone and MDC produced significant elevations in brain extracellular dopamine and 5-HT when administered in vivo. Thus, HHMC, in its unconjugated form, is able to serve as a monoamine transporter substrate, but this metabolite does not normally reach the brain after systemic methylone administration.
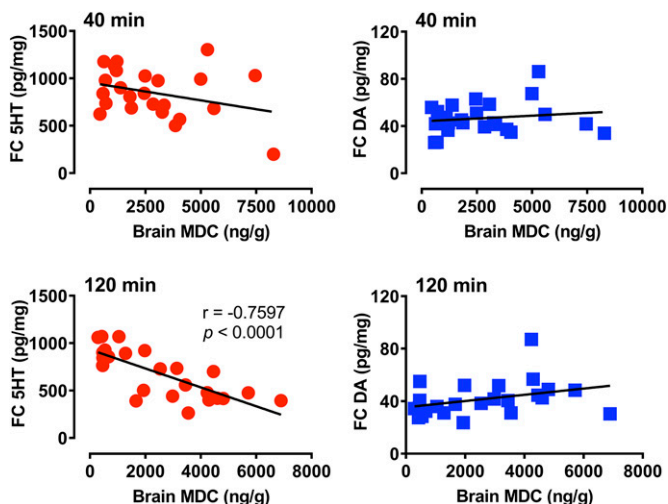

Fig. 11. Correlations between brain MDC concentrations and frontal cortical (FC) 5-HT and dopamine (DA) at 40 and 120 minutes postinjection.

A secondary aim of the present study was to relate pharmacodynamic effects of methylone to brain concentrations of the drug and its metabolites, especially MDC, since this is the main metabolite reaching the brain. The behavioral scoring method that was used to assess locomotor activation is sensitive to dose-dependent changes in behavior induced by stimulant drugs in rats (Elmore et al., 2017). Methylone produced dose-dependent increases in forward locomotion, rearing, and patterned sniffing, consistent with previous reports of its stimulant effects in rats (López-Arnau et al., 2013; Elmore et al., 2017; Štefková et al., 2017; Javadi-Paydar et al., 2018). We found that behavioral scores were positively correlated with brain methylone and MDC concentrations at both time points examined, suggesting these analytes could contribute to motor stimulation. Effects of methylone on core temperature were more complex, characterized by acute hypothermia followed by a delayed, albeit modest, hyperthermia. The effects of methylone administration on body temperature were positively correlated with brain methylone and MDC at 40 minutes, but less so at 120 minutes. In a previous study, Elmore et al. (2017) failed to find any correlation between core temperature and methylone or metabolite concentrations in plasma after subcutaneous injections of 3, 6, or 12 mg/kg. Štefková et al. (2017) observed that methylone significantly increases colonic temperature in individually housed and group-housed rats after subcutaneous doses of 10 and 20 mg/kg, and the effects are maintained for more than an hour. Javadi-Paydar et al. (2018) observed a modest but sustained hyperthermia (0.4–0.8°C) for 4 hours after 10 mg/kg methylone in male rats. Overall, methylone appears to induce modest and sustained hyperthermia in rats, but this effect is influenced by dose and specific experimental conditions.

Perhaps the most important finding in the present report is the acute depletion of brain 5-HT produced by methylone administration. The effects of methylone on tissue 5-HT were dose- and time-dependent, such that the drug produced a delayed decrease in postmortem tissue 5-HT in the frontal cortex but not striatum. The acute effects of methylone on tissue 5-HT reported here are similar to the effects reported for MDMA (Baumann et al., 2007). Previous research has demonstrated that methylone is a nonselective substrate-type releaser at the transporters for dopamine, norepinephrine, and 5-HT (Baumann et al., 2013; Eshleman et al., 2013; Simmler et al., 2013). Like other synthetic cathinones, methylone releases monoamine transmitters from intracellular stores via reversal of normal transporter flux (i.e., reverse transport). The results provided here show that the releasing actions of methylone may lead to acute depletion of intracellular stores of transmitter, but this effect is selective for 5-HT, since postmortem dopamine concentrations are actually increased and not depleted. The 5-HT–depleting action of methylone seems to be exacerbated as time passes, since the most robust effects are observed after 2 hours. We have no explanation for why methylone produces selective decreases in cortical 5-HT, but such reductions could have functional consequences. In animal models, low cerebrospinal fluid concentrations of the 5-HT metabolite 5-HIAA and reduced 5-HT levels or turnover in the brain are associated with increased aggressive behavior (Nelson and Chiavegatto, 2001). In human case studies, methylone overdose is sometimes associated with aggressive and psychotic behaviors, and our preclinical findings suggest that

decreased cortical 5-HT might contribute to such adverse effects (Diestelmann et al., 2018).

In summary, we report the pharmacokinetics of methylone and its three major metabolites in brain and plasma of male rats. Methylone and MDC freely penetrate the blood-brain barrier, whereas HHMC and HMMC do not. Thus, hydroxylated metabolites of methylone do not contribute to centrally mediated pharmacodynamic effects. Methylone and MDC exhibit nonlinear kinetics in the brain when assessed 120 minutes after methylone administration, suggesting delayed accumulation into neurons. Locomotor activity score is positively correlated with brain concentrations of methylone and MDC, whereas postmortem levels of 5-HT in the frontal cortex are negatively correlated with these analytes. Taken together, our findings indicate that nonlinear accumulation of methylone and MDC in the brain could cause untoward effects on 5-HT neurons in vulnerable brain regions, including the frontal cortex.

Authorship Contributions

Participated in research design: Baumann, Concheiro.

Conducted experiments: Centazzo, Chojnacki, Elmore, Rodriguez, Acosta, Baumann.

Contributed new reagents or analytic tools: Suzuki, Rice, Concheiro.

Performed data analysis: Centazzo, Baumann, Concheiro.

Wrote or contributed to the writing of the manuscript: Centazzo, Baumann, Concheiro.

References

Baumann MH, Ayestas MA Jr, Partilla JS, Sink JR, Shulgin AT, Daley PF, Brandt SD, Rothman RB, Ruoho AE, and Cozzi NV (2012) The designer methcathinone analogs, mephedrone and methylone, are substrates for monoamine transporters in brain tissue. *Neuropsychopharmacology* **37**:1192–1203.
Baumann MH, Partilla JS, and Lehner KR (2013) Psychoactive "bath salts": not so soothing. *Eur J Pharmacol* **698**:1–5.
Baumann MH, Raley TJ, Partilla JS, and Rothman RB (1993) Biosynthesis of dopamine and serotonin in the rat brain after repeated cocaine injections: a microdissection mapping study. *Synapse* **14**:40–50.
Baumann MH, Walters HM, Niello M, and Sitte HH (2018) Neuropharmacology of synthetic cathinones. *Handb Exp Pharmacol* **252**:113–142.
Baumann MH, Wang X, and Rothman RB (2007) 3,4-Methylenedioxymethamphetamine (MDMA) neurotoxicity in rats: a reappraisal of past and present findings. *Psychopharmacology (Berl)* **189**:407–424.
Cawrse BM, Levine B, Jufer RA, Fowler DR, Vorce SP, Dickson AJ, and Holler JM (2012) Distribution of methylone in four postmortem cases. *J Anal Toxicol* **36**:434–439.
De Felice LJ, Glennon RA, and Negus SS (2014) Synthetic cathinones: chemical phylogeny, physiology, and neuropharmacology. *Life Sci* **97**:20–26.
de la Torre R, Farré M, Roset PN, Pizarro N, Abanades S, Segura M, Segura J, and Camí J (2004) Human pharmacology of MDMA: pharmacokinetics, metabolism, and disposition. *Ther Drug Monit* **26**:137–144.
Diestelmann M, Zangl A, Herrle I, Koch E, Graw M, and Paul LD (2018) MDPV in forensic routine cases: psychotic and aggressive behavior in relation to plasma concentrations. *Forensic Sci Int* **283**:72–84.
Drug Enforcement Administration (DEA) (2013) Schedules of controlled substances: placement of methylone into schedule I. *Fed Regist* **78**:21818–21825.
Drug Enforcement Administration (DEA) (2019) 3,4-Methylenedioxymethcathinone, Methylone. https://www.deadiversion.usdoj.gov/drug_chem_info/methylone.pdf
Ellefsen KN, Concheiro M, Suzuki M, Rice KC, Elmore JS, Baumann MH, and Huestis MA (2015) Quantification of methylone and metabolites in rat and human plasma by liquid chromatography-tandem mass spectrometry. *Forensic Toxicol* **33**:202–212.

Elmore JS, Dillon-Carter O, Partilla JS, Ellefsen KN, Concheiro M, Suzuki M, Rice KC, Huestis MA, and Baumann MH (2017) Pharmacokinetic profiles and pharmacodynamic effects for methylone and its metabolites in rats. *Neuropsychopharmacology* **42**:649–660.
Eshleman AJ, Wolfrum KM, Hatfield MG, Johnson RA, Murphy KV, and Janowsky A (2013) Substituted methcathinones differ in transporter and receptor interactions. *Biochem Pharmacol* **85**:1803–1815.
Gannon BM, Galindo KI, Mesmin MP, Rice KC, and Collins GT (2018) Reinforcing effects of binary mixtures of common bath salt constituents: studies with 3,4-methylenedioxypyrovalerone (MDPV), 3,4-methylenedioxymethcathinone (methylone), and caffeine in rats. *Neuropsychopharmacology* **43**:761–769.
Gannon BM, Mesmin MP, Sulima A, Rice KC, and Collins GT (2019) Behavioral economic analysis of the reinforcing effects of "bath salts" mixtures: studies with MDPV, methylone, and caffeine in male Sprague-Dawley rats. *Psychopharmacology (Berl)* **236**:1031–1041.
Grecco GG, Kisor DF, Magura JS, and Sprague JE (2017) Impact of common clandestine structural modifications on synthetic cathinone "bath salt" pharmacokinetics. *Toxicol Appl Pharmacol* **328**:18–24.
Javadi-Paydar M, Nguyen JD, Vandewater SA, Dickerson TJ, and Taffe MA (2018) Locomotor and reinforcing effects of pentedrone, pentylone and methylone in rats. *Neuropharmacology* **134**:57–64.
Kamata HT, Shima N, Zaitsu K, Kamata T, Miki A, Nishikawa M, Katagi M, and Tsuchihashi H (2006) Metabolism of the recently encountered designer drug, methylone, in humans and rats. *Xenobiotica* **36**:709–723.
López-Arnau R, Martínez-Clemente J, Carbó Ml, Pubill D, Escubedo E, and Camarasa J (2013) An integrated pharmacokinetic and pharmacodynamic study of a new drug of abuse, methylone, a synthetic cathinone sold as "bath salts". *Prog Neuropsychopharmacol Biol Psychiatry* **45**:64–72.
Luethi D, Kolaczynska KE, Walter M, Suzuki M, Rice KC, Blough BE, Hoener MC, Baumann MH, and Liechti ME (2019) Metabolites of the ring-substituted stimulants MDMA, methylone and MDPV differentially affect human monoaminergic systems. *J Psychopharmacol* **33**:831–841.
Madras BK (2016) The growing problem of new psychoactive substances (NPS), in *Neuropharmacology of New Psychoactive Substances (NPS). Current Topics in Behavioral Neurosciences* (Baumann MH, Glennon R, and Wiley J eds) pp 1–18, Springer, Cham, Switzerland.
Malpass A, White JM, Irvine RJ, Somogyi AA, and Bochner F (1999) Acute toxicity of 3,4-methylenedioxymethamphetamine (MDMA) in Sprague-Dawley and Dark Agouti rats. *Pharmacol Biochem Behav* **64**:29–34.
Meyer MR, Wilhelm J, Peters FT, and Maurer HH (2010) Beta-keto amphetamines: studies on the metabolism of the designer drug mephedrone and toxicological detection of mephedrone, butylone, and methylone in urine using gas chromatography-mass spectrometry. *Anal Bioanal Chem* **397**:1225–1233.
Nelson RJ and Chiavegatto S (2001) Molecular basis of aggression. *Trends Neurosci* **24**:713–719.
Oliver CF, Palamar JJ, Salomone A, Simmons SJ, Philogene-Khalid HL, Stokes-McCloskey N, and Rawls SM (2019) Synthetic cathinone adulteration of illegal drugs. *Psychopharmacology (Berl)* **236**:869–879.
Pedersen AJ, Petersen TH, and Linnet K (2013) In vitro metabolism and pharmacokinetic studies on methylone. *Drug Metab Dispos* **41**:1247–1255.
Schindler CW, Thorndike EB, Goldberg SR, Lehner KR, Cozzi NV, Brandt SD, and Baumann MH (2016) Reinforcing and neurochemical effects of the "bath salts" constituents 3,4-methylenedioxypyrovalerone (MDPV) and 3,4-methylenedioxy-N-methylcathinone (methylone) in male rats. *Psychopharmacology (Berl)* **233**:1981–1990.
Simmler LD, Buser TA, Donzelli M, Schramm Y, Dieu LH, Huwyler J, Chaboz S, Hoener MC, and Liechti ME (2013) Pharmacological characterization of designer cathinones in vitro. *Br J Pharmacol* **168**:458–470.
Štefková K, Židková M, Horsley RR, Pinterová N, Šíchová K, Uttl L, Balíková M, Danda H, Kuchař M, and Páleníček T (2017) Pharmacokinetic, ambulatory, and hyperthermic effects of 3,4-methylenedioxy-n-methylcathinone (Methylone) in rats. *Front Psychiatry* **8**:232.
Vandewater SA, Creehan KM, and Taffe MA (2015) Intravenous self-administration of entactogen-class stimulants in male rats. *Neuropharmacology* **99**:538–545.
Watterson LR, Hood L, Sewalia K, Tomek SE, Yahn S, Johnson CT, Wegner S, Blough BE, Marusich JA, and Olive MF (2012) The reinforcing and rewarding effects of methylone, a synthetic cathinone commonly found in "bath salts". *J Addict Res Ther* (Suppl 9):002.

Address correspondence to: Dr. Michael H. Baumann, Designer Drug Research Unit (DDRU), IRP, NIDA, NIH, DHHS, 333 Cassell Drive, Suite 4400, Baltimore, MD 21224. E-mail: mbaumann@mail.nih.gov; or Dr. Marta Concheiro, Department of Sciences, John Jay College of Criminal Justice, City University of New York, 524 West 59th Street – Rm 5.66.02, New York, NY 10019. E-mail: mconcheiro-guisan@jjay.cuny.edu